

Reconfigurable Design and Modeling of an Underwater Superlimb for Diving Assistance

Jiayu Huo, Jingran Wang, Yuqin Guo, Wanghongjie Qiu, Mingdong Chen, Harry Asada, Fang Wan,* and Chaoyang Song*

This study presents the design of an underwater superlimb as a wearable robot, providing divers with mobility assistance and freeing their hands for manipulating tools underwater. The wearable design features a thrust vectoring system with two 3D-printed, waterproofed modules. The module with adjustable connections and strapping holes is designed to enable reconfiguration for multiple purposes, including regular use as an underwater superlimb for divers, manually operated as a handheld glider for swimmers, combined with an amphibian, legged robot as a quadruped superlimb, and coupled as a dual-unit autonomous underwater vehicle for underwater navigation. The kinematics and dynamics of the prototype and all of its reconfigured modes are developed. A sliding-mode controller is also introduced to achieve stable simulation in PyBullet. Field tests further support the feasibility of the underwater superlimb when worn on a test diver in a swimming pool. As the first underwater superlimb presented in the literature, this study opens new doors for supernumerary robotic limbs in underwater scenarios with multifunctional reconfiguration.

handhelds, mostly lacking an appropriate level of intelligence and autonomy while interacting with humans or the environment.^[2] Wearable devices, such as fins and weights, help divers navigate in 3D. Handheld devices, such as cameras and tools, are mainly used for underwater manual operation, inspection, and maintenance. However, some assistive propulsion devices can also enhance efficiency in aquatic locomotion but occupy the body limbs during operations. In professional diving, divers must focus on engaging with life-supporting wearables while dexterously operating wearable or handheld devices for 3D posture control with 6° of freedom and task-specific operations simultaneously.

The supernumerary robotic limbs, or superlimbs for short, emerge as a novel wearable robot and hold the potential to provide intelligent assistance to divers with


multiple tasks at hand. Superlimbs are generally wearable systems to alleviate the cognitive burden of human limbs while simultaneously interacting with the physical environments in multiple tasks. As a wearable device, superlimbs are distinctively different from prosthetics and exoskeletons in design and human–robot interactions. In general, prosthetics work with human subjects that have lost their physical limbs, therefore focusing on replacing the lost motor functions. The exoskeletons mainly deal with scenarios where the limbs are still presented,

1. Introduction

Besides maintaining life support, a key challenge for self-contained underwater breathing apparatus (SCUBA) diving for commercial purposes under the water is the simultaneous efforts paid to posture balance and 6D spatial movement while conducting task-specific operations by hands.^[1] It is worth noting that life support wearables take a significant portion of divers' devices. The SCUBA gears can be classified into wearables and

J. Huo, J. Wang
Shenzhen Key Laboratory of Intelligent Robotics and Flexible Manufacturing
Southern University of Science and Technology
Shenzhen, Guangdong 518055, China

J. Huo, J. Wang, Y. Guo, W. Qiu, M. Chen, C. Song
Department of Mechanical and Energy Engineering
Southern University of Science and Technology
Shenzhen, Guangdong 518055, China
E-mail: songcy@iee.org

 The ORCID identification number(s) for the author(s) of this article can be found under <https://doi.org/10.1002/aisy.202300245>.

© 2023 The Authors. Advanced Intelligent Systems published by Wiley-VCH GmbH. This is an open access article under the terms of the Creative Commons Attribution License, which permits use, distribution and reproduction in any medium, provided the original work is properly cited.

DOI: 10.1002/aisy.202300245

H. Asada
Department of Mechanical Engineering
Massachusetts Institute of Technology
Cambridge, MA 02139, USA

F. Wan
School of Design
Southern University of Science and Technology
Shenzhen, Guangdong 518055, China
E-mail: wanf@sustech.edu.cn

C. Song
Guangdong Provincial Key Laboratory of Human-Augmentation and Rehabilitation Robotics in Universities
Southern University of Science and Technology
Shenzhen, Guangdong 518055, China

aiming at either enhancing their existing motor functions to exceed their typical performance or regaining the weakened motor functions to match their regular performances.^[3] However, superlimbs interact with human subjects in scenarios where the limbs need to operate multiple tasks at the same time, suitable in either industrial settings, such as overhanging screw-driving,^[4] or home settings, including helping hemiplegia patients eat meals^[5] and providing sit-to-stand assistance for the elderly.^[6]

Breathing, moving, and task-specific operations while underwater are challenging for humans. When submerged underwater, we suffer from significantly reduced sensory feedback caused by the water temperature, clarity of sight, and diving depth. Divers must use various equipment for air supply, including the SCUBA system and the air tank worn on the body. Moreover, the movement underwater is in 3D, which is different from on-land locomotion in 2D. Therefore, a combination of all four body limbs with devices such as fins, gloves, and weights are usually involved underwater, yet the speed of movement is much reduced. The hands are mostly occupied for posture control underwater, making it a difficult task to spare them for tool operation or task completion. The protective glove and waterproof modifications to the conventional tools are additional challenges for manual processes by hand. Besides challenges in the musculoskeletal interaction underwater, the even more significant difficulties are on the cognitive side caused by the diving responses in respiratory, cardiac, and vascular aspects, which may cause further stress to divers with reduced senses underwater.

Many devices and tools have been developed for diving, mainly wearable in design, besides various air supply equipment, protective body suits, and gloves. For example, Nakashima^[7] developed a simulation model for swimming with diving fins, the most common wearable for generating propulsion underwater using periodic leg swing motion. Minak^[8] proposed the experimental method to systematically evaluate the performance of free-diving fins, mainly used for diving at around 100 m in depth. Wearable devices for real-time monitoring of the ECG signals are also developed for emergency alerts in SCUBA diving.^[9] Recent literature also presents the development of a breathing detection system for SCUBA divers.^[10] A recent review on wearable systems for enhancing human movement underwater lists a range of devices for divers.^[11] Among commercial products, the diver propulsion wearables are usually propulsion units attached to the body limbs. When connected to the lower limbs,^[12,13] the divers' hands can be accessible for manual operations but still requires manual control for human-machine interactions. To summarize, these wearables are primarily mechanical by design with a limited advancement in intelligence, mainly for safety assurance and payload reduction without interactions between humans and devices. There exists research that focuses on human-robot interactions in underwater environments, including passing messages from the robot to divers by signaling movements set in advance,^[14] and manipulation of the robot done by the diver using tablets, markers, or gestures as signal inputs,^[15] which must be handled by the diver and keep their hands occupied. Therefore, there remains a research gap in underwater superlimbs for divers with hands-free operation and intention recognition for intelligent human-robot interactions in underwater wearable devices.

In this study, we propose the engineering design of a reconfigurable underwater superlimb for diving assistance, capable of further reconfiguration into various modes of aquatic interaction with human divers, underwater robots, or standalone as an autonomous underwater vehicle (AUV). We present the theoretical modeling of the reconfigurable underwater superlimb and further extend the model into various modes using simulation with a sliding-mode controller, including as a superlimb for human divers, as a superlimb for robot divers, as a handheld device for divers or swimmers, and combined as a standalone AUV, as shown in **Figure 1**. We also conducted preliminary tests in a swimming pool to verify its basic functionalities as an underwater superlimb. Our study demonstrates the design feasibility of such a hybrid and reconfigurable system in a compact form factor with multiple functionalities, paving the path for future integration with intention recognition for human-robot interaction of the underwater superlimb. Note that in this study, we confine our investigation to professional SCUBA diving for commercial purposes only, which is different from commercial diving that utilizes a surface-supplied diving system (SSA), which consists of lengthy, colored hoses (umbilicals) connecting from a gas supply source on the surface to the diver's helmet.

The rest is organized as the following. Section 2 presents the engineering design, theoretical modeling, and sliding-mode control of the reconfigurable underwater superlimb system. Section 3 presents simulation results of the reconfigurable underwater superlimb in various modes and movements and the preliminary field test results in a swimming pool. Section 4 discusses the results of this study and summarizes the conclusion. The limitations and future work are in the final section.

2. The Reconfigurable Underwater Superlimb

2.1. Reconfigurable Engineering Design

Although concepts for underwater propulsion are not new, most existing designs mainly focus on being an exoskeleton instead of a superlimb, where the diver's limbs are still occupied during the process. Instead, we refer to those developed for on-land scenarios to guide the engineering design process, which usually considers attachment to the human or robot body for object manipulation. For on-land scenarios, including overhead tool handling,^[16] manual operation with body support,^[17] or assistive daily-life activities,^[18] the human body is free from existing devices, making the superlimb as the only wearable additional to the human body. Recent research also shows superlimbs with a soft design to provide passive compliance while manipulating objects.^[19]

The underwater scenario also challenges the design of superlimbs, mainly caused by the existing wearables on divers for life support and the spatial body movement in 3D space during diving. During SCUBA diving, the diver's upper body is usually equipped with various devices, including the wet suit, air tank, and regulators, all attached to the buoyancy control device, or BCD, an inflatable jacket worn on the diver's upper body. Once inflated, the BCD becomes tightly attached to the diver's upper body so that the air tanks, tubing, and regulators can

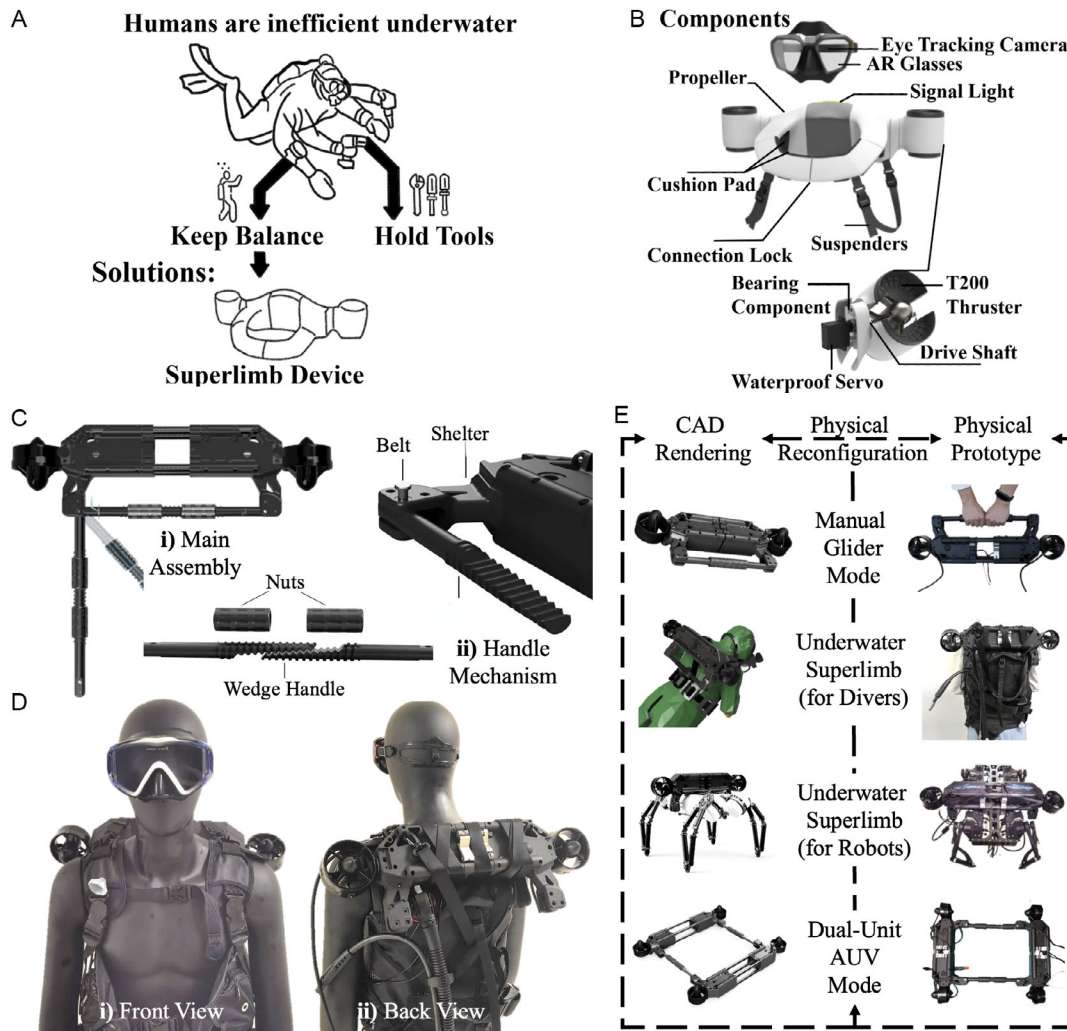


Figure 1. Reconfigurable design of the proposed underwater superlimb for supernumerary diving assistance. A) The technical diving challenge involves simultaneous hand motion to maintain 6D posture balance and conduct underwater task-specific operations. B) The original design concept for an underwater superlimb with directional propulsion. C) The engineering prototype i) in the main assembly view and ii) the handle mechanism with nuts and wedge handles capable of reconfiguration. D) The underwater superlimb worn on a manikin in i) front and ii) back views. E) The four reconfiguration modes are presented in CAD rendering and physical prototypes.

be firmly fixed in an organized manner with minor interference with the body limbs.^[20] During diving, all limbs must work together to achieve successful and smooth body movement with 6°-of-freedom, including descending/floating/ascending vertically, cruising forward/backward, and turning left/right horizontally, which are usually simple and standard for on-land scenarios but become difficult underwater. Other challenging movements, such as moving while facing upside down, flipping with the back facing the ocean floor, or even helical movement that combines spinning about the body axis while moving forward, may become necessary during diving but impossible to achieve on land.

Therefore, we propose the reconfigurable underwater superlimb as a wearable propulsion system with thrust vectoring that can be strapped to the diver's shoulders on the BCD, as shown in **Figure 2A**. We designed the width to be adjustable through the four carbon fiber tubes to fit different divers' shoulder sizes. As shown in **Figure 2B**, each module is designed with through

holes to strap to the BCD hooks easily. Supplementary material includes a video clip of the wearing process. Each module contains a set of 3D printed shells, where the servo (Dynamixel XW540-T140-R) inside the shells is coupled with a thruster (Blue Robotics T200) outside in **Figure 2C**. We used bearings and oil seals for waterproofing and added a silicone sealant along the shell's inner edge to enhance waterproofing, as shown in **Figure 2D,E**.

Furthermore, we designed the superlimb reconfigurable with four multifunctional modes. The CAD rendering and physical prototype of its various modes are shown on the left and right columns of **Figure 1E**. The handheld glider mode is the simplest, where the user grabs the wedge handle to operate the thrusters for efficient movement manually. As a wearable device, the prototype can work as a superlimb for human or robotic divers. As an underwater superlimb for divers, the prototype can be attached to the shoulder of BCD to spare the hands for tool

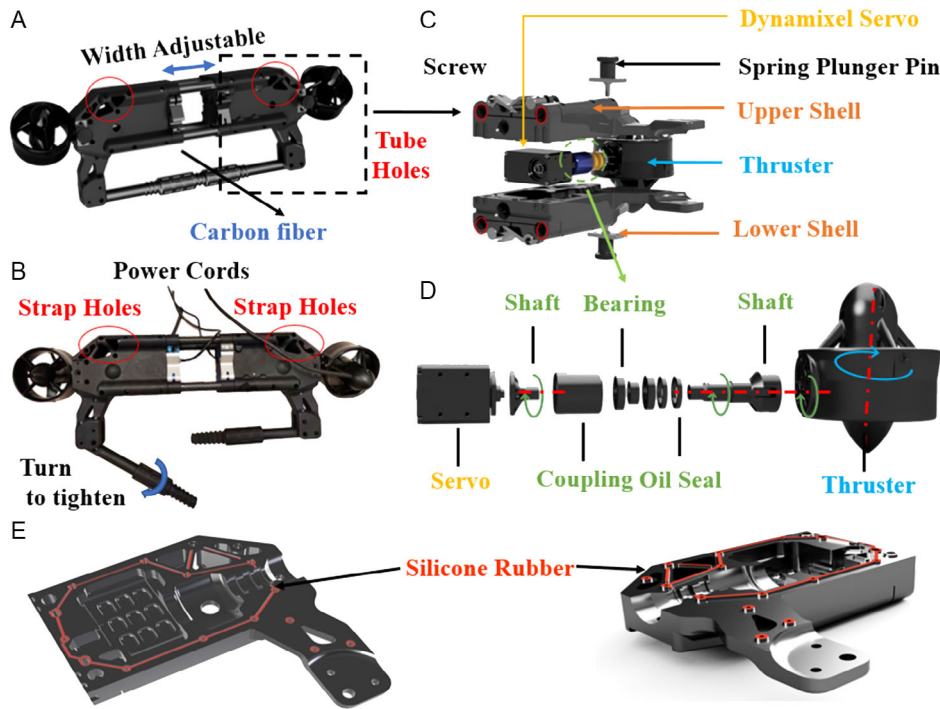


Figure 2. Engineering design of the reconfigurable underwater superlimb module. A) CAD illustration of underwater superlimb with adjustable width with thrust vectoring. B) The strap holes on the engineering prototype for wearing on the BCD. C) The drive unit in an exploded view, including the 3D-printed upper and lower shelters and the thrust vectoring module. D) The thrust vectoring module using a servo (Dynamixel XW540-T140-R) coupled with a thruster (Blue Robotics T200). E) Waterproofing using customized sealant between the upper and lower shelters.

handling. It can also work with a robot diver, such as an amphibian, legged robot,^[21] to provide similar supernumerary robotic assistance. With the wedge handles and rotating bars, two unit models can be mechanically connected to formulate a standalone AUV.

2.2. Theoretical Modeling

The modeling process starts with the reconfigurable unit model as the basis for deriving the other modes of the prototype. Figure 3A marks the coordinate frames, and those for the rest of the modes are shown in Figure 3B–E. We derived the kinematics and dynamics by adapting the bicopter model in ref. [22], which shares similar features of thrust vectoring using servos and brushless motors.

2.2.1. Reconfigurable Unit Model

We set up coordination frame \mathcal{B} of the reconfigurable unit model using u , v , and w axes in Figure 3A. Two frames, \mathcal{T}_1 and \mathcal{T}_2 , are attached to the two thrusters with the origins, O_1 and O_2 , coincide with the servo's rotating axes at a distance d symmetrical to the origin of \mathcal{B} at O_0 . Here, d relates to the adjustable width shown in Figure 2A. The thrusters generate propulsion forces of λ_1 and λ_2 , with the servo angles rotating by θ_1 and θ_2 , respectively.

Based on Newton's and Euler's equations of motion, we set up the dynamics of the translational and rotational motions.

$$\begin{bmatrix} M\mathbf{E}_3\ddot{\mathbf{r}} \\ \mathbf{I}\dot{\boldsymbol{\omega}} \end{bmatrix} = \begin{bmatrix} -M(\mathbf{g} - \mathbf{B}) \\ -\boldsymbol{\omega} \times \mathbf{I}\boldsymbol{\omega} \end{bmatrix} + \begin{bmatrix} \mathbf{R} & \mathbf{O}_{3 \times 3} \\ \mathbf{O}_{3 \times 3} & \mathbf{E}_3 \end{bmatrix} \begin{bmatrix} \mathbf{f} \\ \boldsymbol{\tau} \end{bmatrix} + \mathbf{D} \quad (1)$$

where M denotes the mass of the reconfigurable unit model and \mathbf{I} is its moment of inertia matrix. \mathbf{g} and \mathbf{B} , respectively, denote the gravitational vector and the buoyancy vector. \mathbf{R} is the rotation matrix of the subject, and \mathbf{E} is the rotation matrix of the reconfigurable unit model expressed by Euler angles. \mathbf{r} and $\boldsymbol{\omega}$ denote the position and angular velocity of the subject in the world frame, respectively.

In Equation (1), $[\mathbf{f}^T \ \boldsymbol{\tau}^T]^T$ is the combined forces and torques generated by the reconfigurable unit model defined below

$$\begin{bmatrix} \mathbf{f} \\ \boldsymbol{\tau} \end{bmatrix} = \begin{bmatrix} \mathbf{f}_{\text{load}} \\ \boldsymbol{\tau}_{\text{load}} \end{bmatrix} + \begin{bmatrix} \mathbf{f}_{\text{thrust}} \\ \boldsymbol{\tau}_{\text{thrust}} \end{bmatrix} \quad (2)$$

where $[\mathbf{f}_{\text{thrust}}^T \ \boldsymbol{\tau}_{\text{thrust}}^T]^T$ and $[\mathbf{f}_{\text{load}}^T \ \boldsymbol{\tau}_{\text{load}}^T]^T$ are the forces and torques applied separately to the reconfigurable unit model by itself or the payloads, depending on the specific mode of interaction reconfigured from the unit model.

We also consider the effects of hydrodynamic loads for underwater scenarios by introducing \mathbf{D} in Equation (1), which denotes the matrix of hydrodynamic loads of the reconfigurable model. It also involves two parts, including \mathbf{D}_s applied on the center of mass of the superlimb and \mathbf{D}_{load} as those of the payload, as the following

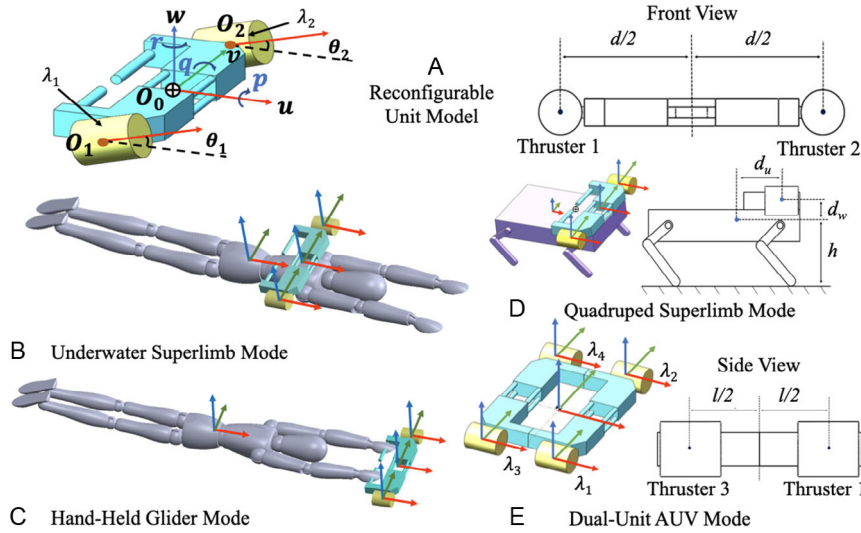


Figure 3. Theoretical modeling of the proposed underwater superlimb, reconfigurable into four modes. A) The reconfigurable unit model and the coordinate frames for modelings. B) The underwater superlimb mode with a simplified CAD model of a human diver. C) The handheld glider mode held by the hands of the simplified diver model for manual operation. D) The quadrupeled superlimb mode wearable on the back of a robot diver (an amphibian, legged robot in this case). E) The dual-unit AUV mode with two reconfigurable units joined on the wedge handles.

$$\mathbf{D} = \mathbf{D}_s + \mathbf{D}_{load} \quad (3)$$

For ease of simulating underwater actions later, we set the buoyancy coefficient to be of the same magnitude but in opposite directions to the gravitational terms, resulting in neutral buoyancy for our models.

$$\mathbf{g} - \mathbf{B} = 0 \quad (4)$$

This simplification is only used in upcoming simulation experiments because the buoyancy will change significantly in an underwater environment at varying depths, including snorkeling and moving long distances. Further detailed modeling would be required.

2.2.2. Underwater Superlimb Mode

While adapting the theoretical model of the reconfigurable unit to other modes of the engineering prototype, we assume the force and torque terms provided by the thrusters and the hydrodynamic loads remain unchanged, which can be modeled as the following

$$\begin{bmatrix} f_u^{Superlimb} \\ f_v^{Superlimb} \\ f_w^{Superlimb} \\ \tau_p^{Superlimb} \\ \tau_q^{Superlimb} \\ \tau_r^{Superlimb} \end{bmatrix} = \begin{bmatrix} \lambda_1 \cos \theta_1 + \lambda_2 \cos \theta_2 \\ 0 \\ \lambda_1 \sin \theta_1 + \lambda_2 \sin \theta_2 \\ (-\lambda_1 \sin \theta_1 + \lambda_2 \sin \theta_2) \frac{d}{2} \\ 0 \\ (\lambda_1 \cos \theta_1 - \lambda_2 \cos \theta_2) \frac{d}{2} \end{bmatrix} \quad (5)$$

Note that in Equation (5), f_u , f_v , and f_w , respectively, denote forces applied in the surge, sway, and heave directions, and τ_p , τ_q , τ_r denote torques applied in the roll, pitch, and yaw directions.

The dominant behavior of hydrodynamic loads applied on the superlimb at low velocities can be captured by quadratic equation.^[23] Therefore, $\mathbf{D}_s^{Superlimb}$ can be written as

$$\mathbf{D}_s^{Superlimb} = - \begin{bmatrix} f_d^u \\ f_d^v \\ f_d^w \\ \tau_d^p \\ \tau_d^q \\ \tau_d^r \end{bmatrix} = - \begin{bmatrix} a_d^u \dot{u} + b_d^u \dot{u}^2 \\ a_d^v \dot{v} + b_d^v \dot{v}^2 \\ a_d^w \dot{w} + b_d^w \dot{w}^2 \\ a_d^p \dot{p} + b_d^p \dot{p}^2 \\ a_d^q \dot{q} + b_d^q \dot{q}^2 \\ a_d^r \dot{r} + b_d^r \dot{r}^2 \end{bmatrix} \quad (6)$$

where \dot{u} , \dot{v} , and \dot{w} are surge, sway, and heave linear velocities, while \dot{p} , \dot{q} , and \dot{r} are roll, pitch, and yaw velocities. a_d and b_d denote linear and quadratic coefficients in corresponding directions for the superlimb, which are modeled similarly in all reconfigured modes.

When working as an underwater superlimb for divers in Figure 3B, $[\mathbf{f}_{load}^{Superlimb} \ \boldsymbol{\tau}_{load}^{Superlimb}]^T$ and $\mathbf{D}_{load}^{Superlimb}$ will be determined by the human diver. In this scenario, we simplify the model by treating the human diver as a rigid body with simple movement to model the hydrodynamics for surge, heave, and yaw displacements. Hence, the forces and torques applied by payloads will be written as the following

$$\begin{bmatrix} \mathbf{f}_{load}^{Superlimb} \\ \boldsymbol{\tau}_{load}^{Superlimb} \end{bmatrix} = [f_{load}^u \ 0 \ f_{load}^w \ 0 \ 0 \ \tau_{load}^r]^T \quad (7)$$

where f_{load}^u and f_{load}^w denote forces applied by diver in axes u and w , and τ_{load}^r denotes the torque in yaw direction.

For simplification, the model of the human diver will be considered with a uniform cross section in all directions involved, indicating that the hydrodynamic loads applied on the diver

could share the same model with Equation (6) but with a_d and b_d replaced by a_{load} and b_{load} , which denote the linear and quadratic coefficients derived from the model of diver.

2.3. Modeling for Reconfiguration

Besides the superlimb for the diver, the reconfigurable unit model can be adapted into the other three modes, including the handheld glider mode in Figure 3C, quadruped superlimb mode in Figure 3D, and dual-unit AUV mode in Figure 3E. Dynamic modeling of these three modes can also be derived from the reconfigurable unit model. To ease the presentation, we only retain those related physical variables. To simplify the hydrodynamics, we also streamline loads of robot and human divers as rigid bodies with uniform cross-sectional areas during movement.

2.3.1. Handheld Glider Mode

This is the simplest mode, manually held by the diver or swimmer by hands, providing assistive propulsion in the surge, yaw, and roll movements, which shares the same model with Equation (5), only with force in heave direction considered 0. For the forces and torques generated by the diver, we consider the model as the following

$$\begin{bmatrix} \mathbf{f}_{load}^{HandHeld} \\ \boldsymbol{\tau}_{load}^{HandHeld} \end{bmatrix} = [f_{load}^u \quad 0 \quad 0 \quad \tau_{load}^p \quad 0 \quad \tau_{load}^r]^T \quad (8)$$

2.3.2. Quadruped Superlimb Mode

Similar to the underwater superlimb mode, the reconfigurable unit could be alternatively fixed on the back of an amphibian, legged robot as a robot driver in Figure 3D. The superlimb can help prevent the robot diver from pitching, assisting it in moving forward and backward along the u -axis and turning on a horizontal plane. Therefore, $\begin{bmatrix} \mathbf{f}_{thrust}^{Quadruped} \\ \boldsymbol{\tau}_{thrust}^{Quadruped} \end{bmatrix}^T$ for the forces and torques of superlimb can be derived from Equation (5) but with f_w and τ_u considered 0. Additionally, τ_v is rewritten as the following

$$\tau_v = \sum_{i=1}^2 (d_u \lambda_i \sin \theta_i + d_w \lambda_i \cos \theta_i) \quad (9)$$

where d_u and d_w are the horizontal and vertical distances between the thruster and the centroid of the whole.

Forces and torques generated by the quadruped robot can be considered as the following

$$\begin{bmatrix} \mathbf{f}_{load}^{Quadruped} \\ \boldsymbol{\tau}_{load}^{Quadruped} \end{bmatrix} = [f_{load}^u \quad 0 \quad 0 \quad 0 \quad hf_{load}^u \quad \tau_{load}^r]^T \quad (10)$$

where h denotes the vertical distance between the centroid and the ground, and f_{load}^u contains the generated force from the legged robot and the friction between it and the ground.

2.3.3. Dual-Unit AUV Mode

When two reconfigurable units are connected on the wedge handles, we get a new robot in the dual-unit AUV mode, where four thrusters work simultaneously to provide 6D movement for the robot.

$$\begin{bmatrix} \mathbf{f}_{thrust}^{DualUnit} \\ \boldsymbol{\tau}_{thrust}^{DualUnit} \end{bmatrix} = \begin{bmatrix} \sum_{i=1}^4 \lambda_i \cos \theta_i \\ 0 \\ \sum_{i=1}^4 \lambda_i \sin \theta_i \\ \frac{d}{2} \sum_{i=1}^4 (-1)^i \lambda_i \cos \theta_i \\ \frac{1}{2} (-\sum_{i=1}^2 \lambda_i \sin \theta_i + \sum_{i=3}^4 \lambda_i \sin \theta_i) \\ \frac{d}{2} \sum_{i=1}^4 (-1)^{i+1} \lambda_i \cos \theta_i \end{bmatrix} \quad (11)$$

$$\begin{bmatrix} \mathbf{f}_{load}^{DualUnit} \\ \boldsymbol{\tau}_{load}^{DualUnit} \end{bmatrix} = \mathbf{0}_{6 \times 1} \quad (12)$$

It should be noted that the two reconfigurable units are considered as a whole without any extra load, so the \mathbf{f}_{load} and $\boldsymbol{\tau}_{load}$ are neglected for this mode. However, one can add a further payload to the center of the robot in this mode, which is essentially empty and can be further fixed with payloads for material transportation underwater.

2.4. Determining the Coefficients

2.4.1. Physical Constants

Table 1 contains the physical parameters of the three model units that appear in the reconfigurable model. Each part's mass, size, and related model parameters are generated using the CAD models. The measured value of the parameter l in the dual-unit AUV mode is 250.00 mm, which is gained by connecting two reconfigurable units.

2.4.2. Hydrodynamic Coefficients

We estimated the coefficients of the hydrodynamic terms by referring to the data from ref. [24], which reported an experimental setup with published measurement of forces under actual flow. We then estimate hydrodynamic parameters based on the data and make adjustments according to the difference between the shape of the AUV in the experiment and that of our model. The coefficients for robot and human divers can be obtained using the same method.

2.5. Sliding-Mode Controller for Simulation

The electronic hardware of the underwater superlimb is shown in Figure 4A, which is waterproofed by the waterproofed acrylic tube, integrated with a depth sensor (MS5837 B30A), a bidirectional ESC for the thrusters, a 9-axis IMU (3DM-GX3-25), and a control unit (Raspberry Pi 4B). The superlimb control was implemented as a sliding-mode Simulink model, illustrated in Figure 4B.

Table 1. Coefficients for theoretical modeling.

Model	Mass [kg]	Size [mm]	Model coeff. [mm]	Axis	Inertia	Linear coeff.	Quadratic coeff.
Reconfigurable unit	3.15	185.00 × 666.14 × 55.50	$d = 546.00$	u		-0.13	18.03
				w		-0.49	67.21
				q		0.08	0.08
				r	0.17	0.45	0.05
Human diver	72.20	1649.32 × 339.14 × 191.00		u		-0.23	31.59
				w		-2.24	305.05
				r	2.00	3.62	0.40
Quadruped robot diver	18.81	500.00 × 350.00 × 100.00	$d_u = 159.32$ $d_w = 66.18$ $h = 267.18$	q	0.87	0.14	1.84

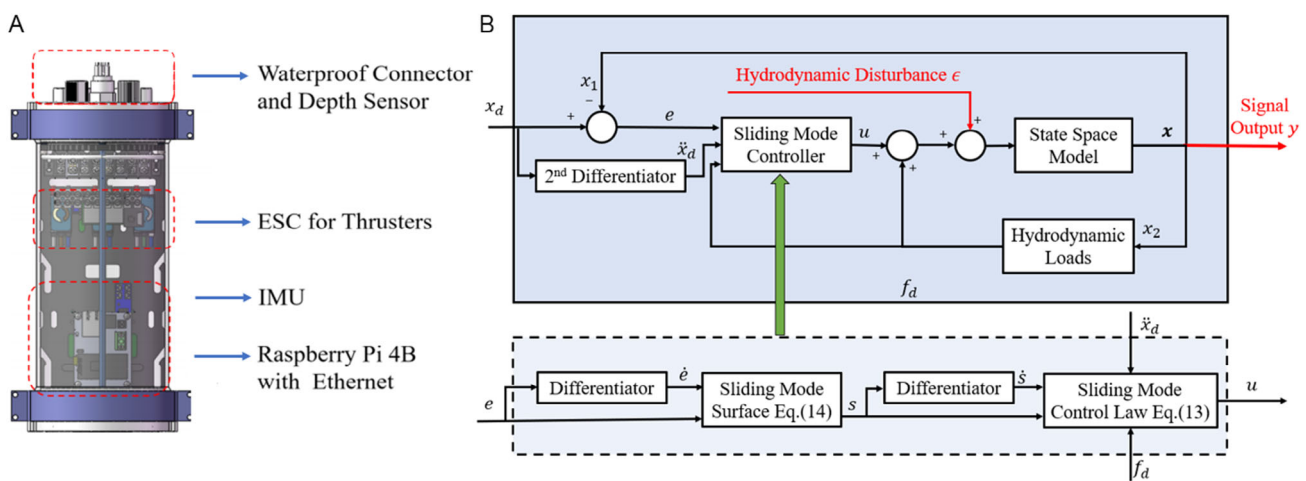


Figure 4. Controller hardware and control system's structure in the simulation of the reconfigurable underwater superlimb. A) Waterproofed electronics hardware for the control unit; B) control diagram with the detailed structure of the sliding-mode controller.

The control law below was based on the process in ref. [25]

$$\mathbf{u} = -\mathbf{D} + \begin{bmatrix} \mathbf{M}\mathbf{E}_3 & \mathbf{O}_{3 \times 3} \\ \mathbf{O}_{3 \times 3} & \mathbf{I} \end{bmatrix} (-C_2\mathbf{s} - C_1\dot{\mathbf{s}} - \mathbf{e} + \ddot{\mathbf{t}}\mathbf{hd}) \quad (13)$$

where \mathbf{u} denotes the input vector provided by thrusters on the superlimb, which can be further derived into thrusts of each thruster by solving Equation (5) or 11; \mathbf{M} and \mathbf{I} are the system's total mass and moment of inertia; \mathbf{D} stands for the hydrodynamic load of the whole body; $\mathbf{t}\mathbf{hd}$ is the desired position; C_1 and C_2 are the parameters that need to be adjusted; \mathbf{e} denotes the state error in the system; and \mathbf{s} denotes the sliding surface, which in this case is given by $\mathbf{s} = \dot{\mathbf{e}} + C_1\mathbf{e}$.

3. Experiment Results

3.1. Simulation of the Reconfigurable Unit Model

3.1.1. Simulation Setup

One single superlimb underwater should have three directly controllable degrees of freedom, which can be derived from Equation (1)

$$m_s \dot{u} = f_u - f_d^u + \epsilon_u \quad (14)$$

$$m_s \dot{w} = f_w - f_d^w + \epsilon_w \quad (15)$$

$$I_s \dot{r} = \tau_r - f_d^r + \epsilon_r \quad (16)$$

where ϵ_u , ϵ_w , and ϵ_r are the disturbances applied by sudden waves that are neglected in the experiment below.

3.1.2. Simulation Results

Two simulations are conducted for the reconfigurable unit model in surge and yaw movements.

Surge Experiment: In this experiment, we aim to control speed in the x axis of the superlimb. By substituting Equation (6) into (14), state space model can be written as

$$\begin{cases} \dot{x}_1 = x_2 \\ \dot{x}_2 = \frac{1}{m} (u - a_d^u x_2 - b_d^u x_2^2) \end{cases} \quad (17)$$

where u denotes the two thruster inputs. By substituting relating parameters shown in Table 1 and entering a unit step input as expected velocity, we conduct experiments focusing on velocity

data within 10 s under six pairs of parameter settings as shown in Figure 5A, where results can be found that when C_1 increases, both rise time and overshoot decrease; when C_2 increases, rise time decreases while the overshoot increases.

Yaw Experiment: Here, we expect the reconfigurable unit to perform angle control for rotation in the yaw direction. Compared to surge and heave experiments, the controller's main structure remains unchanged, while the state space model is obtained from Equation (16) substituted with Equation (5) and (6) as

$$\begin{cases} \dot{x}_1 = x_2 \\ \dot{x}_2 = \frac{1}{I} (u - a_d^r x_2 - b_d^r x_2^2) \end{cases} \quad (18)$$

As shown in Figure 5B-I, results can be found that no overshoot is observed in the experiments involved, and rise time shares a similar performance with experiments conducted above.

3.2. Simulation of the Four Configurations

3.2.1. For the Underwater Superlimb Mode

Here, in the first experiment, we expect the human diver can move along the w -axis to reach an ideal depth with the assistance of the superlimb. In the second experiment, we control the system's rotation around the w -axis by a certain angle. The state-space models here are similar to Equation (17) and (18), with mass, inertia, and hydrodynamic loads updated according to Table 1. The experimental results are shown in Figure 6A. Furthermore, for the robustness justification of the control system, we applied a disturbance as a sudden marine current on the system for depth control, as shown in Figure 6E.

3.2.2. For the Handheld Glider Mode

We assume the human diver moves along the u -axis to reach the desired position. The only difference between this parameter and

the experiment of the underwater superlimb mode is the drag coefficients due to the variation of the superficial area. Results are shown in Figure 6B.

3.2.3. For the Quadruped Superlimb Mode

We started from the horizontal state, aiming at controlling the robot diver to lift its body and reach a stable condition with a specific angle down from the ground in Figure 6C. State-space model of this experiment is similar to Equation (18), with inertia and hydrodynamic loads updated according to Table 1.

3.2.4. For the Dual-Unit AUV Mode

We conducted two experiments in this mode: a yaw angle control similar to Section 3.1 and a heave displacement control, in which a pulse disturbance is applied. State-space models of these experiments are similar to Equation (17) and (18) but with hydrodynamic coefficients, mass and inertia doubled. In Figure 6D and for all six experiments stated above, the effect of C_1 and C_2 is consistent with the yaw experiment of the reconfigurable unit model. For the robustness justification of the control system, we applied a disturbance as a sudden marine current on the system for depth control, as shown in Figure 6F.

3.3. Field Testing in the Pool

We conducted field tests in a swimming pool to verify the feasibility of the prototype's engineering design in providing super-numerary propulsion as a wearable device. We tested the prototype in underwater superlimb mode, in which we strapped the prototype to the test diver's BCD on the shoulder. The prototype is controlled through a computer on land, communicating with the prototype through an Ethernet cable. It provides active modulations of thrust vectoring to help the test diver to achieve simple cruising

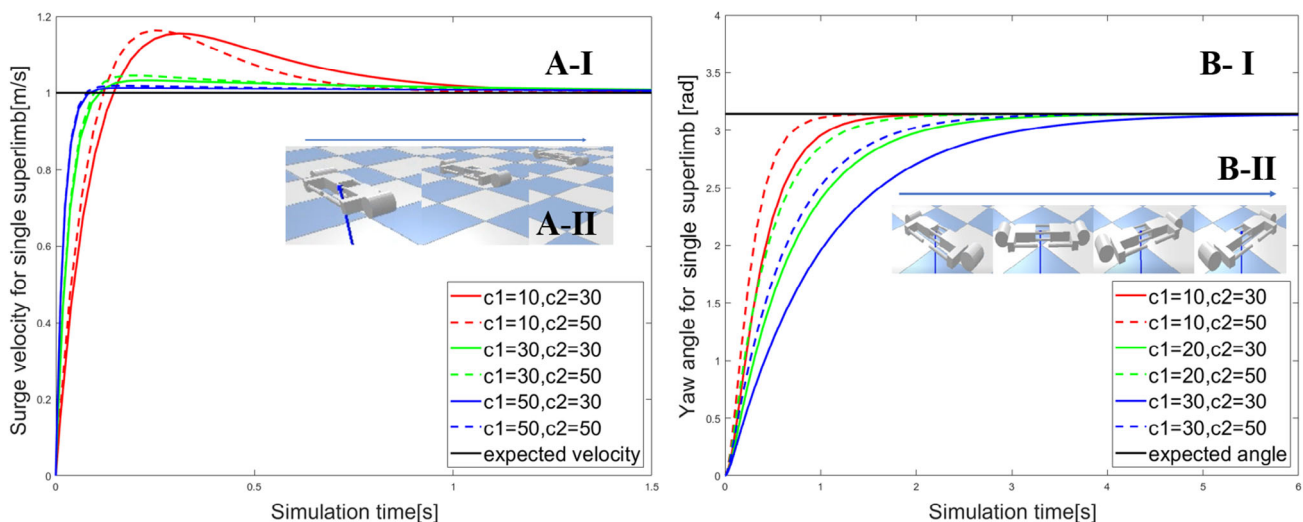


Figure 5. Simulation results in Simulink in MATLAB and PyBullet for the reconfigurable unit model using sliding mode controller. A-I) Surge velocity step response, including the solid and dash lines denoting two settings of C_2 and the other colors denoting three settings of C_1 , and A-II) simulated in PyBullet when given a command to move forward at a speed of 1 m s^{-1} . B-I) Yaw angle step response with the same parameter settings and B-II) simulated in PyBullet when given a command to change the yaw angle by 90° .

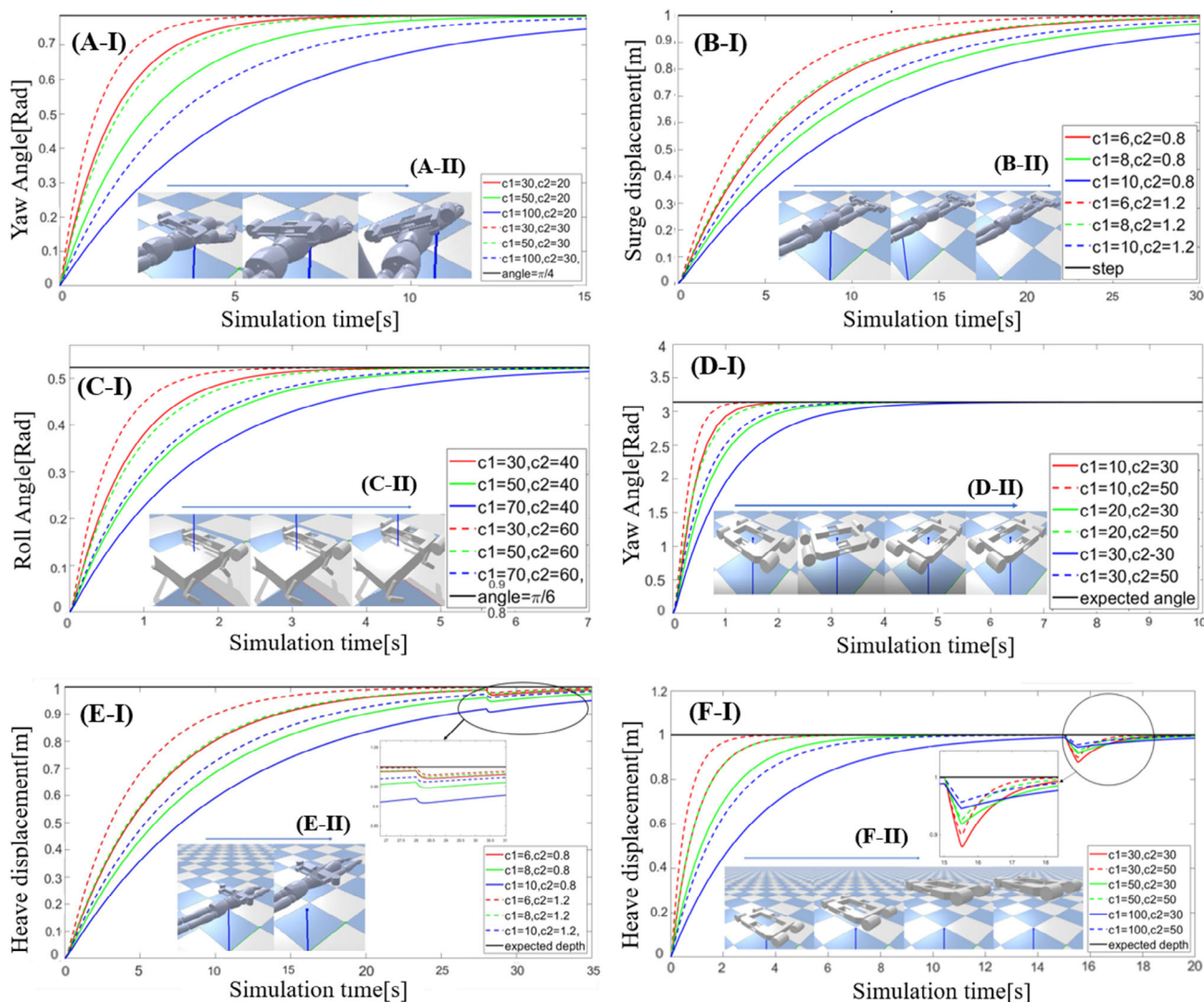


Figure 6. Simulation results for different modes of the superlimb using sliding mode controller. A-I) The underwater superlimb on a human diver in yaw angle control and A-II) simulated in PyBullet when given a command to change yaw direction by 45° . B-I) The handheld glider in surge displacement control with a unit step input and B-II) simulated in PyBullet. C-I) The quadruped superlimb in pitch angle control and C-II) simulated in PyBullet when given a command to change the pitch angle by 30° . D-I) The dual-unit AUV in yaw angle control and D-II) simulated in PyBullet when given a command to change the yaw angle by 90° . E-I) The underwater superlimb on a human diver in heave displacement control with unit step input and E-II) simulated in PyBullet and a disturbance of 150 N for 10 s. F-I) The dual-unit AUV in heave displacement control with unit step input and F-II) simulated in PyBullet when given a command to change the yaw angle by 90° , along with a disturbance of 60 N for 1 s.

forward or turning in directions. The prototype also managed to assist the test diver in achieving other complex movements with at least two motions combined, as shown in **Figure 7**.

During all tests with the underwater superlimb mode, all four limbs of the test diver are free from any movement or operation of tools, which meets the original intention of our design. However, some force must be generated on the waist to comply with the prototype's thrust vectoring propulsion, which indicates potential signals for intention recognition for higher level control, which is beyond the scope of this study and will be addressed in future work.

In addition, due to the limitation of the cable length of the thrusters and servos for the existing engineering prototype and the unavailable of the swimming pool up to date, we cannot conduct the surge experiment for the reconfigurable unit model.

Therefore, we only perform lab testing to validate the control law of the yaw controller for the reconfigurable unit model in a smaller plastic water tank (size: $1.8\text{ m} \times 1.5\text{ m} \times 0.5\text{ m}$). The experiment setup is shown in **Figure 8**, and the experimental results are demonstrated in **Figure 9**.

4. Discussions and Conclusion

4.1. Feasibility Analysis of the Engineering Design

This study presented the reconfigurable design and theoretical modeling of an underwater superlimb for diving assistance, aiming at freeing the diver's hands from posture controls while



Figure 7. Screenshots of field testing for supernumerary diving assistance without using any of his limbs in a swimming pool. A) Helical cruising to move forward while spinning about his body axis. B) Turning with depth control to turn left while diving to the bottom of the pool. C) Cruising with depth control to move forward while diving to the bottom of the pool.

operating tools and exploring new frontiers of wearable robotics with supernumerary assistance in the underwater scenario, which is not yet reported in the current literature to the best of our knowledge.

We proposed a reconfigurable design of the underwater superlimb for multifunctional purposes while being compatible with the BCD jacket as a wearable design. The wearable design features a thrust vectoring system with two 3D-printed, waterproofed modules, each embedded with a servo for directional control and a thruster for propulsion. The connection between the modules and the strapping holes on the modules is specially designed to enable reconfiguration of the system for multiple purposes, including regular use as an underwater superlimb for divers, manually operated as a handheld glider for swimmers, combined with an amphibian, legged robot as a quadruped superlimb, and coupled in a pair as a dual-unit AUV for autonomous navigation underwater. We studied the reconfigurable

modeling of the underwater superlimb through theoretical analysis, simulation investigation, and preliminary field test to verify the feasibility of the concept as a novel robotic system for diver assistance, contributing to the future research of supernumerary robotics in fields other than those on land, which has been well researched in the current literature already.

We also identified differences compared to existing wearable devices for underwater propulsion assistance. For example, the CudaJet^[26] is a well-designed product with powerful propulsion assistance, requiring a handheld controller and cannot provide directional controls for posture adjustment, such as holding positions underwater, which is capable with our design using directional propulsion. The Jet Beluga^[27] is a well-documented project that shares the same problem as the CudaJet. Besides, our study also provides the theoretical analysis and simulation and the reconfigurable capability for multifunctional purposes, which are also fundamentally different.

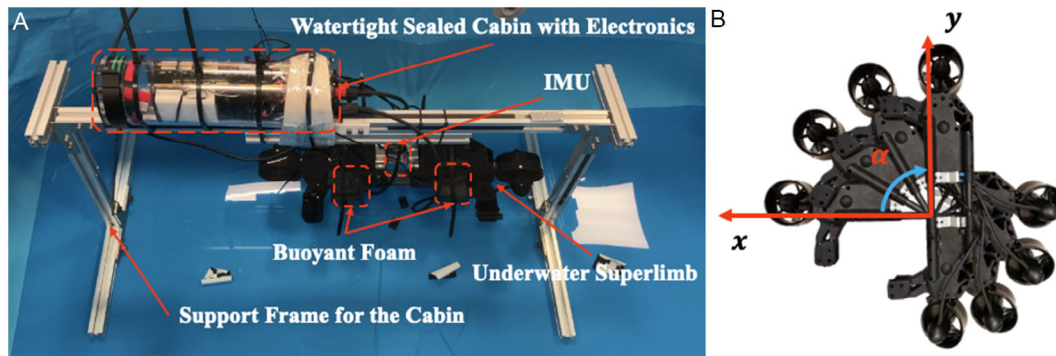


Figure 8. The experiment setup of the yaw control for the underwater superlimb. A) The experiment setup of the superlimb in a pool ($1.8 \times 1.5 \times 0.5$ m), including an IMU sensor with a waterproof shell attached at the center of the superlimb, which can estimate the yaw angle of the superlimb at 100 Hz. The buoyant foams are used to control the buoyancy to ensure the neutral buoyancy state of the superlimb. The support frame for the cabin is needed for the security of the sealed cabin, which is close to the surface of the water to provide enough length of the cable of the thrusters and servos (the cable lengths of the thrusters and servo are limited to 0.7 and 0.6 m, respectively). The electronics control the thrusters and servo according to the command from a PC (Ubuntu) outside of the pool, which undertakes to record the motion data of the superlimb from the IMU sensor, including accelerations and Euler angles. B) The yaw angle definition for the yaw control experiment.

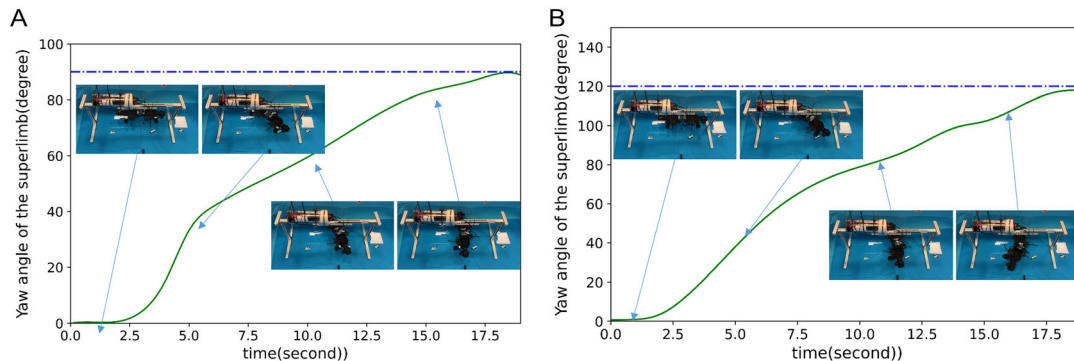


Figure 9. The performance of the yaw control of the underwater superlimb. The solid green line represents the yaw angle value from the IMU sensor, and the blue dotted line represents the step function command of the input signal. A) Given a step signal ($\alpha = \frac{\pi}{2}$) as the input signal to the system, the yaw angle feedback of the superlimb from the IMU sensor. B) Given a step signal ($\alpha = \frac{2\pi}{3}$) as the input signal to the system, the yaw angle feedback of the superlimb from the IMU sensor.

4.2. Reconfigurable Modeling and Simulation

We modeled the underwater superlimb based on similar designs for aerial systems with extended considerations for the underwater scenario. Due to the reconfigurable design, the resultant model can be conveniently remodeled for all configurations of the underwater superlimb. For simulations, results show that the sliding-mode controller can be used as all three motion controllers required, including displacement, angle, and velocity controls. For example, by comparing results from position and velocity control experiments conducted on the reconfigurable unit in Figure 5, it can be inferred that state responses under both control methods can reach the expected stability without adjusting the two parameters.

The change in the dynamic model still creates difficulties in determining parameter settings. In linear position control of dual-unit AUV in Figure 6F, underwater superlimb in Figure 6E, and handheld glider in Figure 6B, the system responds much slower when simulated with the human diver, which takes more than 10 s to reach its goal even if both C_1

and C_2 are significantly lowered. Additionally, the effects on the system response caused by the parameter C_1 still differ between displacement control and velocity control, making it challenging to optimize parameter settings in all motion control simultaneously. In this case, the superlimb requires several parameter settings and the ability to switch flexibly among them to ensure reconfiguration.

Generally speaking, diving activities for commercial or technical purposes are still labor intensive that require an operator submerged underwater, which is not suitable for the biological design of a human. Having a robotic system exploring the underwater environment as a proxy to the human diver is also a viable solution that has been actively explored in recent literature. For example, the Ocean One project by Stanford^[28] is a good example, where they designed a robotic diver as a human diver for underwater archaeological exploration. For practical purposes, adding arms to a standard ROV could be functional for the same purpose. But such a humanoid design opens new doors to human–robot interaction in a challenging environment, similar to how human divers work underwater. The Aquanaut Subsea

Robot developed by HMI^[29] is another example of an underwater robot taking the form of a diver with the added capability to reconfigure into a cruising vessel. It shares similar characteristics as the Ocean One in terms of a humanoid robotic diver design, with added capability for shape transformation.

With our design, we identify a potential direction of future research that leverages the reconfigurable capability of the proposed underwater superlimb to combine with another robotic system as a hybrid and intelligent proxy for human divers or even reconfigurable by itself to become an autonomous agent for underwater tasks. Both serve the same purpose of becoming intelligent agents to replace human divers in such challenging environments underwater.

4.3. Supernumerary Robotic Assistance for Diving

In this study, although intention recognition is yet to be integrated into the proposed prototype, we have conducted field tests of the underwater superlimb to verify its engineering design and primary performance in providing propulsion assistance as wearable underwater when attached to the BCD. As shown in Figure 7, the system can be conveniently strapped to the BCD to become a wearable device for divers. When worn on the shoulder, the test diver successfully performed various basic movements without using the limbs, including simple cruising forward and turning directions. In addition, the test diver can also perform some challenging moves, such as the helical cruising movement that involves cruising forward while spinning about the body axis in Figure 7A, the turning while the diving movement that consists in cruising to the bottom of the pool while turning in directions in Figure 7B, and the simple depth control that helps the diver to reach the bottom of the pool and then to the surface in Figure 7C. For the preliminary testing, we verified the supernumerary assistance provided by the underwater superlimb in generating active propulsion in diving. The overall design worked smoothly and relieved the diver from active movement in the limbs, which validates the design as an underwater superlimb. Also, we validated the feasibility of the control law for the yaw controller of the reconfigurable unit model. Although there are differences between the simulation results and the lab testing results, which is due to the disturbance of the drag force of the thrusters and servo partly, the demonstration in Figure 9 shows that the yaw controller can stable the unit model in about 15 s.

5. Limitations and Future Work

While the engineering feasibility of the underwater superlimb has been verified, this study is also limited in various aspects. For example, the strapping process remains clumsy but can be further improved so that the diver can put it on without help from others. The field test is yet to incorporate autonomous control by an algorithm or manual control by the diver, which requires further communication from another computer on the ground. Moreover, the field tests for other modes of the underwater superlimb after reconfiguration are yet to be conducted.

For future work of this study, we intend to introduce intention recognition into the system by adding sensors to the goggles for detecting throat vibrations and head movements. In simulations, we plan to involve gait control while conducting experiments in the quadruped mode, such as helping the quadruped robot stand straight by two of its four legs, allowing it to move like humanoids while underwater. We also intend to field-test the other modes and improve the wearable design for durability tests. Nevertheless, the results presented in this study open new doors for supernumerary robotics limbs in underwater scenarios with multifunctional reconfiguration.

Supporting Information

Supporting Information is available from the Wiley Online Library or from the author.

Acknowledgements

J.H. and J.W. contributed equally to this work as co-first authors. This work was partly supported by the SUSTech-MIT Joint Centers for Mechanical Engineering Research and Education, the Science, Technology, and Innovation Commission of Shenzhen Municipality (grant nos. ZDSYS20220527171403009, JCYJ20220818100417038, and 20200925155748006), National Natural Science Foundation of China (grant no. 62206119), and Guangdong Provincial Key Laboratory of Human-Augmentation and Rehabilitation Robotics in Universities. The experiment was approved by the Southern University of Science and Technology Internal Review Board (grant no. 20230072). The authors would like to thank Yu Jie, Ziqian Wang, and Feng Tian for assisting in conducting field testing of the underwater superlimb prototype, He Wang, Rongzheng Zhang, and Yuanning Han for preparing the engineering design figures and in-lab testing of the prototype.

Conflict of Interest

The authors declare no conflict of interest.

Data Availability Statement

The data that support the findings of this study are available from the corresponding author upon reasonable request.

Keywords

reconfigurable design, supernumerary robotic limbs, underwater robots, underwater superlimbs

Received: May 11, 2023

Revised: June 12, 2023

Published online:

- [1] E. R. Straughan, *Emotion Space Soc.* **2012**, *5*, 19.
- [2] S. Togawa, N. Yamami, M. Shibayama, H. Nakayama, T. Nozawa, Y. Mano, E. Yoshida, M. Maruyama, *Jpn. J. Sports Med. Phys. Fitness* **2006**, *55*, 341.
- [3] H. Li, D. Sui, H. Ju, Y. An, J. Zhao, Y. Zhu, *IEEE/ASME Trans. Mechatron.* **2022**, *27*, 5392.

- [4] B. L. Bonilla, H. H. Asada, in *IEEE Int. Conf. Robot. Autom. (ICRA)*, IEEE, Piscataway, NJ **2014**, p. 119.
- [5] H. Song, H. H. Asada, *IEEE Rob. Autom. Lett.* **2021**, *6*, 1646.
- [6] X. Wu, H. Liu, Z. Liu, M. Chen, F. Wan, C. Fu, H. Asada, Z. Wang, C. Song, in *IEEE Int. Conf. Soft Robot. (RoboSoft)*, IEEE, Piscataway, NJ **2020**, pp. 599–606.
- [7] M. Nakashima, Y. Tanno, T. Fujimoto, Y. Masutani, *Proceedings* **2018**, *2*, 6.
- [8] G. Minak, *Sports Eng.* **2004**, *7*, 153.
- [9] T. Cibis, B. H. Groh, H. Gatermann, H. Leutheuser, B. M. Eskofier, in *Conf. Proc. IEEE Eng. Med. Biol. Soc. (EMBC)*, IEEE, Piscataway, NJ **2015**, pp. 6074–6077.
- [10] C. Altepe, S. M. Egi, T. Ozyigit, D. R. Sinoplu, A. Marroni, P. Pierleoni, *Sensors* **2017**, *17*, 6.
- [11] H. Xia, M. A. Khan, Z. Li, M. Zhou, *IEEE/CAA J. Autom. Sin.* **2022**, *9*, 967.
- [12] M. J. Thiessen, Underwater Personal Propulsion Device, <https://patents.google.com/patent/US20110174209A1> (accessed: February 2023).
- [13] A. G. Benjamin McGeever, Personal Dive Device with Electronic Speed Control, <https://patents.google.com/patent/US20090249991A1> (accessed: February 2023).
- [14] N. Mišković, A. Pascoal, M. Bibuli, M. Caccia, J. A. Neasham, A. Birk, M. Egi, K. Grammer, A. Marroni, A. Vasilijević, Z. Vukić, in *OCEANS - Aberdeen*, IEEE, Piscataway, NJ, USA **2017**, pp. 1–5.
- [15] A. Birk, *Curr. Rob. Rep.* **2022**, *3*, 199.
- [16] C. Davenport, F. Parietti, H. H. Asada, in *ASME 2012 5th Annual Dynamic Systems and Control Conference (DSCC) joint with the JSME 2012 11th Motion and Vibration Conference*, American Society of Mechanical Engineers, New York, USA **2012**, Vol. 1, pp. 787–793.
- [17] F. Parietti, H. Asada, *IEEE Trans. Rob.* **2016**, *32*, 301.
- [18] P. H. Daniel, C. Fu, H. H. Asada, *IEEE Access* **2022**, *10*, 6814.
- [19] S. Liu, Y. Zhu, Z. Zhang, Z. Fang, J. Tan, J. Peng, C. Song, H. H. Asada, Z. Wang, *IEEE/ASME Trans. Mechatron.* **2021**, *26*, 2747.
- [20] W. Zuo, X. Yi, F. H. Ghorbel, Z. Chen, in *IEEE Conf. Decis. Control (CDC)*, IEEE, Piscataway, NJ, USA **2019**, p. 2120.
- [21] Y. Gu, S. Feng, Y. Guo, F. Wan, J. S. Dai, J. Pan, C. Song, *Mech. Mach. Theory* **2022**, *176*, 105018.
- [22] T. Anzai, Y. Kojio, T. Makabe, K. Okada, M. Inaba, in *IEEE-RAS Int. Conf. Humanoid Robot. (Humanoids)*, IEEE, Piscataway, NJ, USA **2021**, p. 69.
- [23] W. Wang, C. M. Clark, in *OCEANS - Asia Pacific*, IEEE, Piscataway, NJ, USA **2006**, p. 1.
- [24] R. Gabl, T. Davey, Y. Cao, Q. Li, B. Li, K. L. Walker, F. Giorgio-Serchi, S. Araci, A. Kiprakis, A. A. Stokes, D. M. Ingram, *Ocean Eng.* **2021**, *234*, 109279.
- [25] Z. Yan, Z. Yang, J. Zhang, J. Zhou, A. Jiang, X. Du, *IEEE Access* **2019**, *7*, 166788.
- [26] Cudajet, Underwater Jetpack Luxury Superyacht Toy, <https://cudajet.com/products/underwater-jetpack> (accessed: March 2023).
- [27] J. Graham, B. Amaral Neves, E. Genter, Jet Beluga: Diver Propulsion Wearable, <https://openscholarship.wustl.edu/mems411/131> (accessed: March 2023).
- [28] O. Khatib, X. Yeh, G. Brantner, B. Soe, B. Kim, S. Ganguly, H. Stuart, S. Wang, M. Cutkosky, A. Edsinger, P. Mullins, M. Barham, C. R. Voolstra, K. N. Salama, M. L'Hour, V. Creuze, *IEEE Rob. Autom. Mag.* **2016**, *23*, 20.
- [29] J. E. Manley, S. Halpin, N. Radford, M. Ondler, in *OCEANS - Charleston*, IEEE, Piscataway, NJ, USA **2018**, pp. 1–4.